TITLE: Cold Gas Dynamic Manufacturing - A New Approach to Near-Net
Shape Metal Component Fabrication

DISTRIBUTION: Approved for public release, distribution unlimited

This paper is part of the following report:

TITLE: Materials Research Society Symposium Proceedings, Volume 758
Held in Boston, Massachusetts on December 3-5, 2002. Rapid Prototyping
Technologies

To order the complete compilation report, use: ADA417756

The component part is provided here to allow users access to individually authored sections
of proceedings, annals, symposia, etc. However, the component should be considered within
the context of the overall compilation report and not as a stand-alone technical report.

The following component part numbers comprise the compilation report:
ADP014213 thru ADP014236

Cold Gas Dynamic Manufacturing –
A new approach to Near-Net Shape Metal Component Fabrication

R. H. Morgan, C. J. Sutcliffe, J. Pattison, M. Murphy, C. Gallagher,
A. Papworth, P. Fox, W. O'Neill
Manufacturing Science and Engineering Research Centre, Department of Engineering
The University of Liverpool, L69 3GH, UK. r.morgan@liverpool.ac.uk

ABSTRACT

Cold Gas Dynamic Manufacturing (CGDM) is a high-rate, direct deposition process capable of combining many dissimilar materials in the production of a single component. The process is based on Cold Gas Dynamic Spraying (CGDS) – a surface coating technology in which small, un-heated particles are accelerated to high velocities (typically above 500 m/s) in a supersonic gas jet and directed towards a substrate material. The process does not use a heat source (as with similar plasma and HVOF spray technologies), but rather employs the high kinetic energy of the particles to effect bonding through plastic deformation upon impact with the substrate or previously deposited layer. As a consequence it lends itself to the processing of temperature sensitive material systems such as oxidising, phase-sensitive or nano-structured materials. To achieve metallic bonding incident particles require velocities greater than a certain material-specific threshold value, such that thin surface films are ruptured, generating a direct interface. This bonding mechanism has been compared to explosive welding.

This paper discusses the further development of the CGDS technique from surface coating technology into the basis for a novel Additive Fabrication process. The description of the apparatus is presented in addition to the basic processing conditions for the deposition of aluminium material. Particular attention is paid to the morphology of the deposited material, the microstructure and the interfacial boundary between splats.

CURRENT TECHNOLOGY AND LIMITATIONS

Current trends in the area of Rapid Prototyping (RP) and Manufacturing have led to the development of processes which provide end users with metal components which are not simply form and fit prototypes, but allow functional load-bearing testing or actual in-service use.

The enabling technologies such as Laser Engineered Net Shaping (LENS) [1] and Direct Metal Laser Re-Melting (DMLR) [2] use a laser to melt and fuse high strength, high temperature metallic powder particles into a net or neat-net shape solid form on a layer-by-layer basis. The problems associated with such fabrication processes include the high thermally induced stresses generated in the component and also the requirement of high purity inert environments to prevent oxidation during processing [3]. Furthermore, detrimental microstructure and phase changes may occur. Such metallurgic transformations introduce further complications in the fabrication of Functionally Graded Material (FGM) components or the utilisation of novel nanocrystalline powders.

A new fabrication technology currently under development at the University of Liverpool, UK, is Cold Gas Dynamic Manufacturing. This process will enable the fabrication of near-net shape multiple material components at room temperature, with little or no melting, thus preventing many of the problems that are associated with laser based technologies.

The CGDM technique uses a supersonic gas jet to accelerate small diameter (10-50 μm) particles to high velocities in the range 500-1000 ms^{-1}. The particles are directed towards a target surface and upon impact undergo plastic deformation. It is thought that the kinetic energy of the particles is sufficiently high to effect rupture of surface oxide films, resulting in metal-to-metal bonding with a mechanism considered similar to that of explosive welding [4].

Historical perspective

CGDM is an evolutionary progression from Cold Gas Dynamic Spraying (CGDS) or Cold Spray. The origins of Cold Spray date back to the turn of the twentieth century, introduced by Samuel Thurston in 1902 [5]. The process was subsequently re-discovered and a developed into a material coating technology at The Russian Academy of Sciences, Novosibirsk in the 1980s [6]. Scientists conducting supersonic wind tunnel tests observed that above a certain material-specific critical velocity, particles entrained in the fluid stream adhered to a body obstructing the flow. Table I shows the threshold velocities for deposition of a variety of engineering materials.

Material	Critical Deposition Velocity (ms^{-1})
Copper	560-580
Nickel	620-640
Iron	620-640
Aluminium	680-700

Table I. Critical velocities for deposition for various materials.

The potential advantages of the process were quickly realised and steps were undertaken to develop the phenomenon into a material coating process to compete with coating technologies such as thermal spray [7]. Since then, a variety of research institutions and universities have been investigating cold spray, its underlying physical principles and the materials formed. To date, a variety of materials including copper, aluminium, titanium, silver, nickel-based superalloys, metal matrix composites and nanostructured materials have been successfully deposited [8].

The CGDM process takes the principles of Cold Spray and uses it to create discrete features by xy movement of a CNC controlled deposition nozzle above a substrate. Following the deposition of a layer, a high-speed machining spindle is employed to remove excess material deposited by the diverging spray from the nozzle. Subsequent layers are built up using these process steps until the component is complete. This paper details the preliminary results of the work carried out on CGDM.

EXPERIMENTAL ARRANGEMENT

The experimental arrangement for CGDM comprises of the following components: gas delivery; process chamber; gas recovery. These will be discussed in turn:

Gas delivery

In order for the sprayed particles to attain sufficient kinetic energy to undergo plastic deformation upon impact they must be accelerated to very high velocities by the gas jet. Typical process gasses can be air or nitrogen, however low molecular weight gasses such as helium are preferred, as they will achieve higher velocities [9]. The high-pressure gas (15-30 bar) is delivered through a convergent-divergent nozzle, such as that shown in figure 1, to achieve supersonic velocity. The design of such a nozzle is briefly described below.

Nozzle design

Using quasi one-dimensional flow theory, assuming adiabatic, inviscid gas, the flow can be described as isentropic and hence any change in pressure will be accompanied by a change in density. Under this assumption, the area-velocity relation can be achieved [10]. When applying this relation to subsonic flow (M<1), a decrease in area will result in an increase in velocity (and vice versa), whereas in supersonic flow (M>1), an increase in velocity is associated with an increase in area.
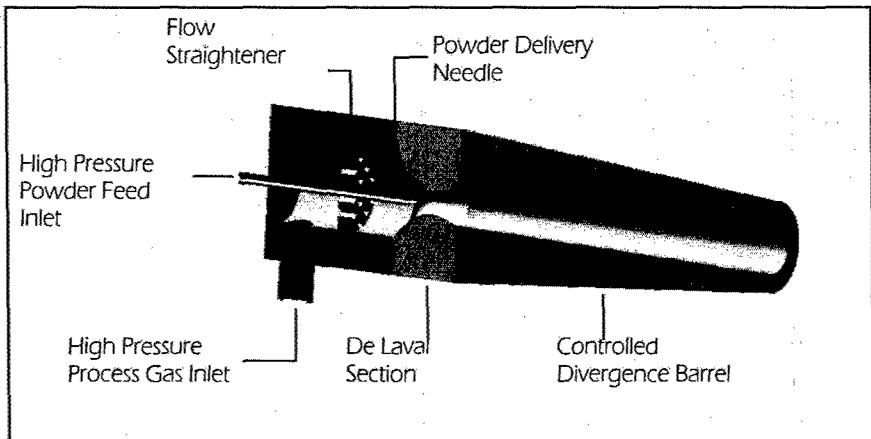
Figure 1. Illustration of nozzle used in Cold Gas Dynamic Manufacturing process.

In the convergent subsonic flow section of a De Laval nozzle, the velocity increases up to the throat, at which point the flow becomes choked (M=1). Immediately after the throat, as the nozzle diverges, the expansion of the gas accelerates the flow to supersonic velocity. Using the Mach number relation through a variable area duct [10], the nozzle exit area can be determined for a particular throat diameter and desired Mach number at a given input pressure and temperature for a particular gas or gas mix. By this method, an axi-symmetric De Laval section has been designed for an output Mach number of 2.4 with helium as the process gas at an input stagnation pressure of 15 bar.

This approach, however, will lead only to the gas velocity and not the more important particle velocity. The particles entrained in the gas jet are much more massive than the gas

molecules and therefore have too much inertia to keep up with the sudden gas acceleration [11]. The particles do accelerate, due to the drag force imposed upon them by the high velocity gas. The drag force on a particle accelerating through the nozzle is given by the equation:

$$F = C_d.A.(\frac{1}{2}\rho.V_{rel}^2) \tag{1}$$

where C_d is the skin friction drag coefficient, A is the cross sectional area of a particle and $1/2\rho V_{rel}^2$ is the dynamic pressure of gas stream relative to the particle

In order for the particles to achieve to their critical velocity, the longer time they spend in the high-speed gas stream the faster their ultimate velocity. Therefore, the divergence length of the nozzle must be optimised to achieve maximum acceleration of the particles. If the divergence length is too short, the particles will not reach their critical velocity. If the nozzle length is too long however, increasing boundary layer effects of the nozzle wall will slow down the gas stream [12].

To optimise the length of the divergence, a series of numerical simulations utilising an industry standard CFD package with a state of the art discrete phase modeller was undertaken. The results of the CFD predictions of the centre-line Mach number can be seen in figure 2. From the throat (x = 0.00), gas velocity is rapidly accelerated to a maximum, maintaining a high velocity just below 1400m/s along the length of the divergence until the nozzle exit is reached. Upon exiting the nozzle, the gas again expands slightly resulting in an increase in velocity. Once the jet is in the atmosphere, viscous forces rapidly entrain atmospheric air, dissipating energy and
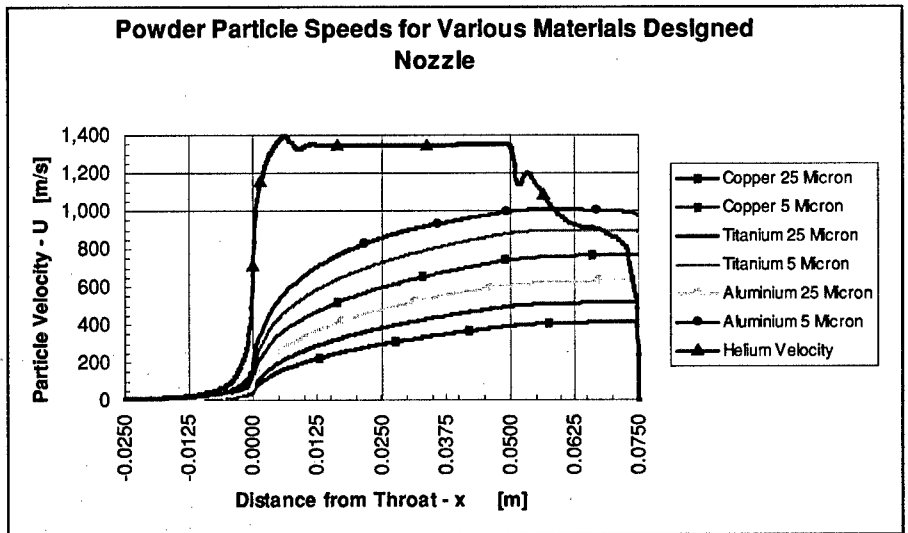

Figure 2. Predictions of gas velocity and velocities of 3 materials at 5 μm and 25 μm particle size.

abruptly reducing the gas velocity. Finally, the jet impacts the substrate plate and is decelerated to almost zero velocity in the axial direction. Particles entrained in the high velocity flow are accelerated steadily along the nozzle length. In fact, the particles continue to accelerate outside the nozzle exit as they still occupy a region in the flow where the relative gas velocity continues to have an impact on the drag force as described by equation 1.

Figure 2 clearly shows the influence of particle size on velocity. In general, small particles with low mass will achieve higher velocities. However, there are limitations to the size of particles; small particles are highly explosive due to their high surface energy, they also tend to agglomerate to form larger particle groups and their surface oxide to volume ratio is increased. Furthermore, the effect of "bow shock" will decelerate smaller, lighter particles. As the gas jet impinges on the substrate surface, a shock wave is formed directly opposing the flow, resulting in a region of stagnation. The decelerating effect of the bow shock on the smaller, lighter Al particles can be seen in figure 2 as they near the substrate.

Process chamber and gas recovery

Powder is fed into the nozzle via a high-pressure gravity feeder (Praxair 1264HP). A perforated spinning disk within the feeder is rotated at a particular speed to set powder mass flow rate. The powder is delivered into the high-pressure convergent section of the nozzle via a tube. The small diameter powders are extremely explosive if exposed to an oxidising atmosphere, therefore, the process chamber is kept inert and the gas and any un-adhered powder are collected. The Initial design for this collection system is shown in figure 3. A clear PU cylinder with a flexible PTFE seal around its base allow the nozzle and chamber to slide as one along a ground base plate
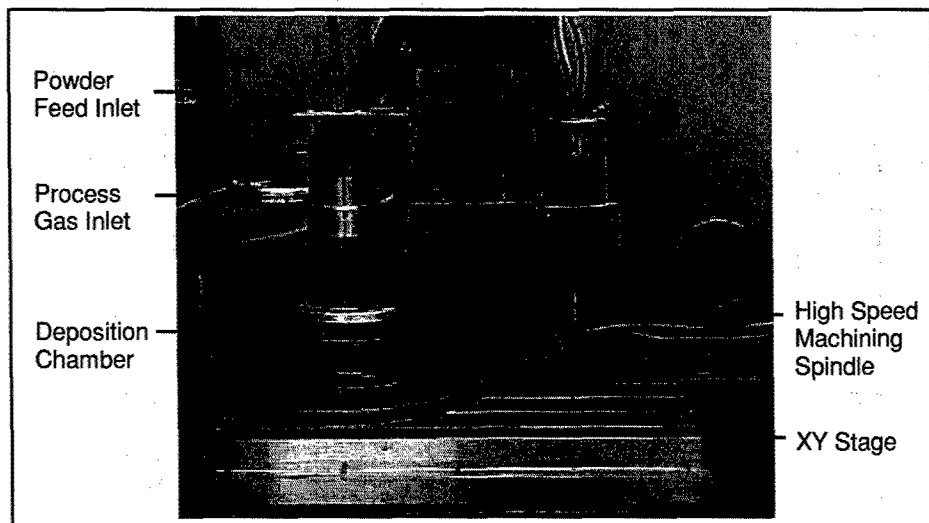
Figure 3. Experimental arrangement incorporating process control chamber and high speed machining spindle.

effectively providing a moveable inert chamber. The chamber exhausts into a scrubbing system consisting of various cyclone and membrane filters, which remove the particles before the gas is exhausted to atmosphere outside the laboratory. Due to the high gas consumption, gas recovery will become an important issue for Cold Spray processes. Work is currently being carried out in this field by industrial collaborators BOC Gases.

RESULTS

Material deposition

The material used in this study is, gas atomised, spherical, pure (industrial grade) aluminium powder supplied by Aluminium Power Company, UK. The powder size is specified as −10 + 45 μm. From table I, the critical deposition velocity of aluminium is 680-700 m/s. Though this is a particularly high threshold velocity, the low material density of aluminium (2.7 g/cm^3) results in its low inertia and hence ease of acceleration.

The main process variables of pressure, nozzle standoff distance, traverse speed and powder mass flow rate were analysed for optimisation of material deposition; table II lists the variable ranges. Figure 4 shows a typical series of deposit tracks on an Al substrate.

| Process Parameter	Variable Range
Process Gas Pressure	11 – 22.5 bar
Nozzle Stand Of Distance	10 – 50 mm
Powder mass flow rate	12.5 – 52.5 g/min
Nozzle traverse rate	50 – 400 mm/min

Table II. Process parameters investigated in CGDM deposition trials.

The results of the deposition trials are extensive and beyond the general nature of this paper. However, the effects of the process variables can be generalised as follows:

Input Gas pressure: Deposition was achieved throughout all input stagnation pressures suggesting critical velocity was achieved. Particles in the centre of the gas stream reach higher velocities than those on the outer edges resulting in a central peak along the length of the deposits, as can be seen in figure 4. Track width increases with pressure as the velocity distribution of the gas jet outside the nozzle is increased, resulting in particles at the extremities of the spray achieving the critical deposition velocity.

Stand Off Distance: Stand off distance contributes greatly to the width of a deposit due to the increase in divergence of the spray. Similarly, the diverging spray also leads to a reduction in deposition height as the deposited powder is spread over a larger area. There is a maximum stand off distance of 50mm beyond which deposition falls off dramatically. This is due to continued deceleration of the particles over a greater length outside the nozzle.

Powder mass flow rate: As powder mass flow rate is increased, the deposition track height increases. At first this occurs rapidly, then reaching a maximum at 45 g/min. Beyond this mass flow rate, excess powder loading within the nozzle causes chocking at the throat and acceleration is less efficient resulting in a limited deposition.
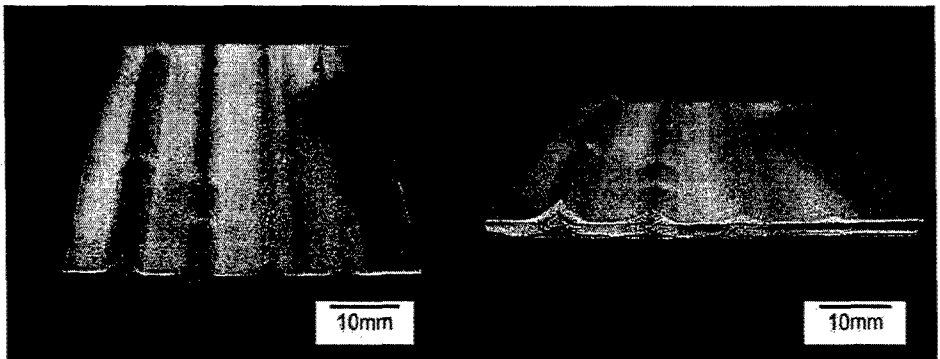
Figure 4. Typical experimental array of single-pass tracks deposited by CGDM:
Constants: Pressure (P) =14 bar, Standoff (h) = 40 mm, Powder mass flow rate (m) = 15 g/min.
Traverse speed (L-R): 1 = 50 mm/min, 2 = 100 mm/min, 3 = 250 mm/min, 4 = 500 mm/min.

Traverse Speed: Figure 4 is an example of the effects of traverse speed. As is expected, the deposition height is a function of the powder deposited per unit length, and therefore an increase in traverse speed leads to a decrease in deposition thickness.

These simple analyses of deposition are important to the development of a near-net shape manufacturing system. As can be seen, the peaked profile of the deposits will result in poor edge definition and optimisation of spray overlap is under investigation. Also, the development of 2D profile nozzles is under investigation to provide flatter deposit profile. However, of overriding importance to the successful production of components by this route is the structural integrity and material characteristics of the deposit.

Microstructural analysis of deposits

Samples were prepared using standard metallographic techniques and etched with 1% NaO_3 solution. Figure 5a shows the typical microstructure. The image reveals splat morphologies significantly different from the shape of the feedstock; the aspect ratio of the impacted particles being substantially higher than that of the spherical, gas atomised powders. This suggests that the material is undergoing significant deformation upon impaction. The amount of deformation results in low porosity in the deposit. However, dark interfacial lines between the splats are apparent. This suggests that metallic bonding is not occurring and that oxide films still exist.

Figure 5b shows the same deposit etched for a greater length of time to emphasise the interfaces between splats. There is little evidence throughout the samples of interfacial bonding taking place. The boundaries between splats have grown significantly, further supporting evidence of poor bonding.

Figure 6 shows SEM images of single particle impacts. Here, significant deformation of the spherical particles can be seen. Evidence of jetting can be seen around the edges of particles. Crater formation of the substrate is also visible in some instances.

79
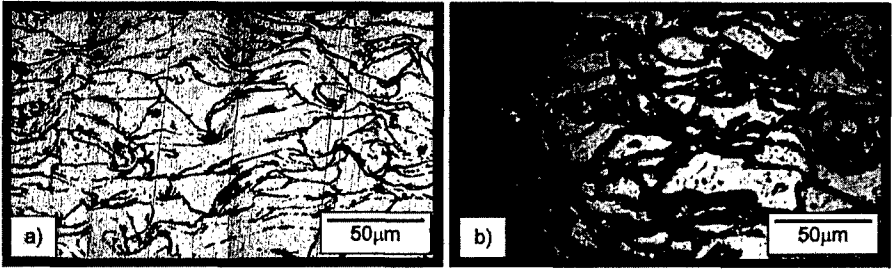
Figure 5. Microstructure of Al deposit – a) Splat morphology shows particles have undergone significant deformation; b) Interfaces between splats have enlarged suggesting no metallic bonding has occurred.
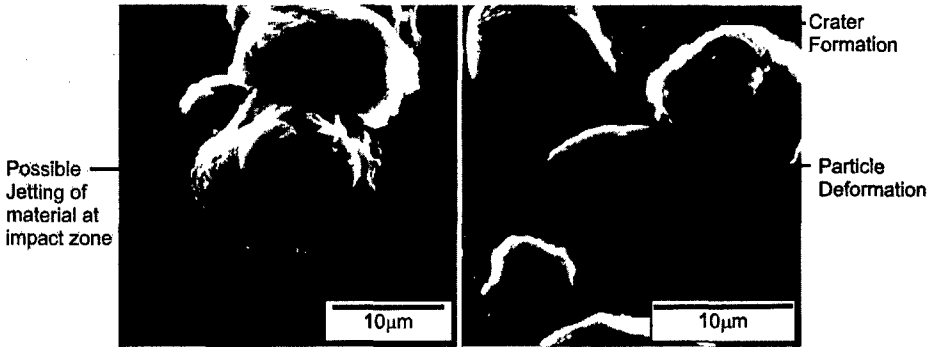

Figure 6. SEM image of Al particles impacted on polished steel substrate. Particle deformation and possible jetting is evident. The formation of an impact crater is also visible in the right hand image.

Auger Electron Spectroscopy (AES) analysis of a deposit sample fractured under high vacuum reveals high oxygen content across the fracture surface, as shown in figure 7. Here, the peaks of C, O_2 and Al are clear. Figure 8 shows the same sample surface after ion beam milling. The milling rate was 7 Å/min. After 45 minutes, the oxygen and carbon spectra are almost completely removed, inferring an oxide thickness of 31 nm (Figure 8).

Discussion

The initial deposition trials have provided a means of identifying the important process parameters for CGDM in terms of deposition rate and deposition thickness. There are, however, a number of issues that need addressing before the technique can be successfully applied to manufacturing.

80
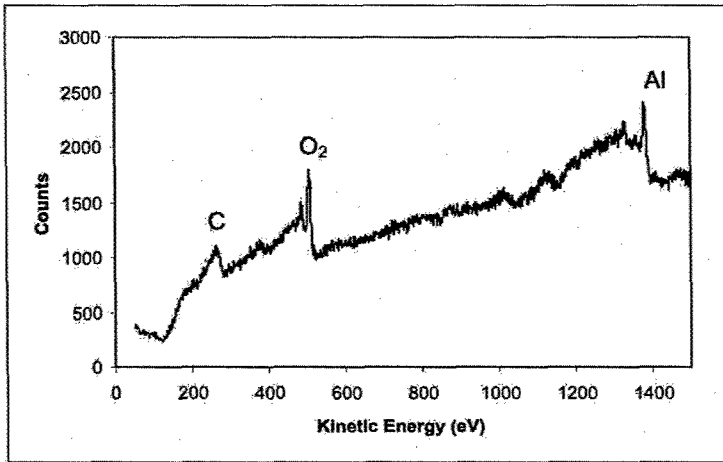
Figure 7. Auger Electron Spectroscopy of CGDM fractured surface. Fractured under vacuum, the sample exhibits carbon, oxygen and aluminium spectra from the surface.
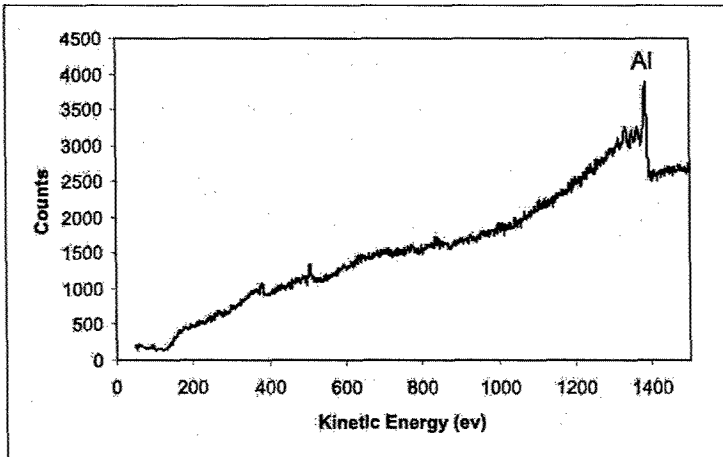
Figure 8. Auger Electron Spectroscopy of CGDM fractured surface. Fractured under vacuum, the sample surface is ion-beam milled for 45 min at a rate of 7 Å/min. The carbon and oxygen contaminants have been removed from the sample surface.

The shape characteristics of the deposit will be an important factor in determining the performance of the process. The peaked shape of the deposits will inevitably lead to poor edge definition and will consequently have an impact on minimum feature size and shape in component fabrication, because of this, a certain degree of back machining of the deposit will be

required. The ratio of material removal to deposited material will also have an impact on the viability of the process, as will the effect of the machining process on the material properties.

A more fundamental issue to be addressed is the properties of the deposited material. The mechanisms of adhesion in cold spray deposition are still not fully understood. Van Steenkiste *et al* identify three possible candidate mechanisms for bonding [13]. If the velocity of the particles is sufficient to exceed yield stress upon collision, then adhesion through plastic deformation will occur. Figure 5 shows the structure of the material exhibits substantial deformation of the particles upon impact, while SEM analysis supports this with evidence of particle deformation and crater formation of the substrate.

The second mechanism for adhesion may be through partial melting and fusion of the material upon impact. The occurrence of jetting may indicate that the material undergoes a kinetic to thermal energy transition leading to softening or partial melting. This has been observed by other researchers and has also been predicted by modelling of the impact zone with temperatures in excess of 900 K, of the order of the melt temperature of aluminium [14, 15].

The third mechanism for particle-particle/substrate adhesion is through fracture of the oxide such that metal-metal bonding can occur. The particles would require a further increase in velocity for this bonding mechanism to take place [13].

In the work reported here, it is clear that particles are undergoing deformation. However, the analysis of the microstructure suggests that interfacial bonding is not being achieved; rather, there is conformal deformation of the particles with the pre-deposited material and mechanical interlocking is taking place. Auger spectroscopy supports this through the detection of carbon and oxygen spectra from the fracture surface. Also, the ion-beam milling of the surface results in removal of these peaks after 31 nm. This depth corresponds with the typical oxide thickness for commercial, passivated powders (20-40 nm). From this, it can be surmised that the particles are not achieving the critical velocity to effect metallic bonding through rupture of the oxide film.

Higher particle velocities can be achieved through an increase in gas velocity. Increasing gas pressure will do this, but at the expense of increased gas consumption and rapidly diminishing returns. A more effective method is to raise the gas temperature. The local sonic velocity in the throat of the nozzle is related to the specific gas properties according to the relationship:

$$V_g = \sqrt{\gamma R T_g} \tag{2}$$

where γ is the ratio of specific heats, R is the specific gas constant and T is the gas temperature in the throat. Thus an increase in gas temperature will bring about a proportional increase in gas and hence particle velocities. To this end, the CGDM apparatus is undergoing modification for the inclusion of gas heating.

The adhesion mechanism in cold spray is still not fully understood. It appears that bonding involves the compaction, deformation, re-orientation and plastic flow of particles under high pressure to break through surface oxides and generate metallic bonds. However, there are many questions still unanswered; how often does metallic bonding occur throughout a cold spray material? What becomes of the pre-existing oxide that resides on the surfaces of the feedstock material? How does this affect the bulk properties of the fabricated material? Can highly oxide-sensitive material be processed successfully for the fabrication of load bearing components? Many other issues also need addressing; the high-energy multiple impacts cold work the material [13], how does this affect the bulk properties? What of the residual stresses in the deposit? For

spray coatings, these issues may not have the same importance as for freeform fabrication, however, it is clear there is a need for a greater understanding of the materials science of cold gas dynamic spraying. To this end work is in progress, both experimentally and theoretically, to provide further insight into the physical mechanisms that take place in order to develop this coating technology as a means of net-shape component fabrication.

CONCLUSIONS

The CGDM process has been shown to hold significant promise for the controlled build up of near net shape components. The process holds significant advantages over thermal based freeform fabrication technologies. This initial study has sought to establish the effect of the main processing variables (Pressure, particle mass flow rate, traverse-speed, nozzle standoff distance) on the resulting deposit shape and structure. Microstructural and SEM analysis of the deposit reveals significant deformation of impacted material. However, further analysis by Auger Electron Spectroscopy has revealed the presence of oxygen across interfacial boundaries suggesting insufficient particle velocities to achieve metallic bonding upon impact. Further experimental and theoretical work is in progress to develop the technology into a freeform net-shape manufacturing technology.

ACKNOWLEGMENTS

REFERENCES

1. M.L. Griffith, M.E. Schlienger, L.D. Harwell, M.S. Oliver, M.D. Baldwin, M.T. Ensz, M. Essien, J. Brooks, C.V. Robino, J.E. Smugeresky, W.H. Hofmeister, M.J. Wert, D.V Nelson, Materials and Design, **20** (2) 1999.
2. R.H. Morgan, A.J. Papworth, C.J. Sutcliffe, P. Fox, W. O'Neill, Journal of Materials Science, **37** (15) 2002
3. C. Hauser, T.H.C. Childs, K.W. Dalgarno, Proc Solid Freeform Fabrication Symposium, University of Texas at Austin, TX. **10** 1999
4. M.F. Smith, J.E. Brockman, R.C. Dykhuzien, D.L. Gilmore, R.A. Neiser, T.J. Roemer, Mat. Res. Soc. Symp. Proc. 542. 1999.
5. News Article, IOM[3] Materials World, **10** (9) 2002
6. A. Papyrin, Adv Mat and Proc. 159 (9) 2001
7. A.P. Alkhimov, A.N. Papyrin, V. F. Kosarev, N.I. Nesterovich, M.M. Shushpanov. US Patent. No 5,302,414 1994
8. J. Karithkeyan, Proc. TSS Cold Spray Conf 2002.
9. D.L. Gilmore, R.C. Dykhuzien, R.A. Neiser, T.J. Roemer, M.F. Smith, Journ Thermal Spray Tech **8** (4) 1999

10. B.S. Massey, Mechanics of Fluids. Van Nostrand Reinhold Publishers. London 1970
11. G.S. Settles, S.T. Geppert. Journ Protective Coatings and Linings, **13** (10) 1996
12. B.R. Munson, D.F. Young, T.H. Okiishi. Fundamentals of Fluid Mechanics. Wiley Publications 1990
13. T.H. Van Steenkiste, J.R. Smith, R.E. Teets, J.J. Moleski, D.W. Gorkiwicz, R.P. Tipson, D.R. Marantz, K.A. Kowalsky, W.L. Riggs II, P.H. Zajchowski, B. Pilsner, R.C. McCune, K.J. Barnett. Surface and Coatings Technology **111** (1) 1999
14. R.C. Dykhuzien, M.F. Smith, D.L. Gilmore, R.A. Neiser, X. Jiang, S. Sampath, Journ Thermal Spray Tech **8** (4) 1999
15. A.N. Papyrin, V.F. Kosarev, S.V. Klinkov, A.P. Alkhimov. Proc Int. Thermal Spray Conf 2002